Electrochemical immunoplatform for the quantification of epithelial extracellular vesicles applied to prostate cancer diagnosis

Emiliano Felici[† 1], Coral González-Martínez[† 2, 3, 4], Teresa Valero Griñán [2, 4, 5,*], Sheila Gato-Zambrano [6], Sirley V. Pereira [1], Martín A. Fernández-Baldo [1,*], Francisco G. Ortega-Sanchez [2,3,4]

[1] *Universidad Nacional de San Luis, Facultad de Química, Bioquímica y Farmacia, Instituto de Química de San Luis, INQUISAL (UNSL - CONICET), Av. Ejército de los Andes 950, San Luis D5700BWS, Argentina.*

[2] *GENYO, Centre for Genomics and Oncological Research, Pfizer/University of Granada/Andalusian Regional Government, PTS Granada, Avenida de la Ilustración 114, Granada 18016, Spain.*

[3] *Laboratory of Genetic Identification, Legal Medicine and Toxicology Department, Faculty of Medicine, University of Granada, Avenida de la Investigación 11, Granada 18071, Spain.*

[4] *Instituto de Investigación Biosanitaria ibs.GRANADA, Avda. de Madrid, 15, Granada 18012, Spain.*

[5] *Department of Medicinal and Organic Chemistry, School of Pharmacy, University of Granada, Campus Cartuja s/n, 18071 Granada, Spain.*

[6] *Seliver Group, Institute of Biomedicine of Seville/ /Hospital, Universitario Virgen del Rocío/CSIC/Universidad de Sevilla, Sevilla, Spain.*

[†] Equal Contribution.

Authors to whom correspondence should be addressed: (e-mail) mbaldo@unsl.edu.ar or tvalero@go.ugr.es

Abstract

Prostate cancer (PCa) is the second most commonly diagnosed cancer in men worldwide, and its early detection is critical for improving patient outcomes through timely and effective treatment. In this work, we present the first electrochemical immunoplatform based on magnetic microbeads (MBs) for the determination of epithelial extracellular vesicles (EpEVs), which are emerging as promising biomarkers for PCa diagnosis and prognosis. The immunoplatform employs MBs functionalized with anti-EpCAM antibodies to selectively capture EpEVs, forming sandwich-type immune complexes that are detected via amperometry at disposable screen-printed carbon electrodes. The method demonstrated a detection limit of 0.4 ng μL^{-1} of EpEVs obtained from PC-3 cell line´s culture, excellent reproducibility (coefficient of variation < 5%), and high selectivity against potential interferences. Comparative analysis with colorimetric immune-magnet ELISA test showed a strong correlation between the two methods, confirming the reliability of the proposed approach. Furthermore, the electrochemical platform provided better precision and a lower limit of detection than the immune magnet ELISA method, indicating its superior analytical performance. Clinical validation using patient samples revealed that the combination of EpEV detection with PSA levels significantly improves the sensitivity and specificity of PCa diagnosis. This novel immunoplatform represents a promising analytical tool for early detection and monitoring of PCa, with potential applications in personalized cancer management.

Keywords: epithelial extracellular vesicles; biomarker; prostate cancer; cancer diagnosis; immunoplatform; electrochemical.

1. Introduction

Prostate cancer (PCa) is the second most common diagnosed cancer in men worldwide and, in Europe, the most frequently diagnosed and the third cause of related cancer deaths [1]. Its prevalence is increasing from 5 % at ages younger than 30 years to 59% in older than 79 years [2]. PCa screening are a useful manner to increase the early diagnosis and to reduce the related deaths [3]. However, one of the side effects of large screening is the overdiagnosis, represented by the 50% of the detected cases [3]. Now a day, screening technology is based on the testing of prostate specific antigen (PSA) which is an androgen-regulated serine protease produced by both prostate epithelial cells and prostate cancer [4]. The principal problem of PSA test is the false-positive result that lead to additional medical procedures, such as a prostate biopsy and its side as infections, pain, and bleeding [5]. This issues are responsible of an intense actual debate regarding PSA as a diagnostic, prognostic and screening tool in PCa and therefore it is important to focus on other biomarkers that can support clinical outcomes and decision making [6].

Extracellular vesicles (EVs) are small nanosized particles rounded by a lipidic double membrane [7]. This EVs are produced for all type of cells and contain specific biomarkers from the cells where were produced [8]. These biomarkers are in general nucleic acid, metabolites, lipid and proteins. In process of cell stress and hypoxia, production ration of extracellular vesicles are significantly increased and as consequence an increment of EVs specific from tumoral environment are dumped into the blood circulation affecting the normal signature of the circulating EVs [9]. EVs are considered an excellent carrier of diagnostic, monitoring and, prognosis biomarkers in solid tumors [10], [11]. There are some works that have addressed for the detection of EVs by electrochemical platforms using different markers, such as integrin αvβ6[12], and different sources, like nano-interdigitated electrodes[13]. Also, a study by Jokerst et al., performed a magnetic microparticles-based strategy for the detection of prostate cancer biomarkers like PSA,

prostatic acid phosphatase, carbonic anhydrase 1, osteonectin, IL-6 soluble receptor, and spondin-2, obtaining an area under the curve of 0.84[14].

But in epithelial tumor like PCa, the identification of epithelial EVs are demonstrating behave as a high accurate biomarker. Epithelial EVs (EpEVs) are characterized for the expression of epithelial biomarker as E-Cadherins, Claudins, Epithelial cell adhesion molecule (EpCAM) among others [15]. Here, we focus on EpCAM biomarker, as it is localized in the cell membrane and works as cell adhesion molecule that functions by mechanically attaching cells to adjacent cells and substrates. Despite it is not specific for PCa, this protein has been highly difunded and represent the most employed biomarker in epithelial tumors, circulating tumor cells and EpEVs. EpCAM positive EVs are being studied and proposed as biomarkers in several solid tumors as Breast Cancer [16], Colon Cancer [17], Lung Cancer [18] and others. In PCa, while EpCAM positive in circulating tumor cells (CTCs) are an excellent biomarker [19], EpCAM positive EVs have been poorly studied diagnostic marker in plasma or serum samples.

In this work, we wanted to evaluate no only the diagnostic value of EpCAM positive EVs but also employ electrochemical sensing as a point of care methodology that can be applied in the clinical practices. Electrochemical immunosensors have specially developed for this kind analysis due that their features such as high sensitivity, ease of operation and low manufacturing cost and miniaturization [20], [21]. In our dual-mode immunosensor, we employ magnetic microparticles (MBs) which shows unique properties that make them handy in a wide range of applications. Into an immune-electrochemical system, MBs enhance sensitivity through efficient capturing, analyte's concentration and easy washing in the presence of external magnetic field [22], [23]. So far, there is not a reported immunosensor developed for the detection of EpCAM + EVs in diagnosis of PCa. Hence, we report the first electrochemical sandwich-type bioassay

for the assessment of EpCAM + EVs in early stages of PCa. Through the immobilization of the capture antibody (monoclonal anti-EpCAM) on HOOC-MBs, its incubation with EVs and specific biotinylated detector antibody (anti-CD81) labelled with a streptavidin horseradish peroxidase (strep-HRP) polymer. The amperometric detection of the affinity reaction was performed using disposable screen-printed carbon electrodes (SPCEs) and the hydroquinone (HQ)/H_2O_2 system. This dual-mode immunosensor was applied to a long cohort of PCa patients to assess the clinical value of these EpEVs.

2. Experimental

2.1. Materials and reagents

HOOC-MBs Dynabeads^{TM} (ThermoFisher, USA), EDC/sulfo-NHS solution, MES buffer, Tris-HCl buffer and ethanolamine solution (Sigma Aldrich, USA) were employed for preparation and functionalisation of the MBs. LNCAP and PC-3 PCs cell lines were obtained from ATCC and grown RPMI medium, supplemented with 10 % of Fetal Bovine Serum (FBS) and 1 % of penicillin/streptomycin solution (P/S) (Gibco, USA). Size exclusion chromatography (SEC) columns with 35 nm pore size qEV2 Columnns (Izon, France). All western blot buffers were prepared with chemical grade reagents. The nitrocellulose membranes and precast gels were adquired in Bio-Rad, UK. All the employed antibodies are described next in the specific sub-section. Printed Electrodes were purchased from Palm Sens, Netherlands.

2.2. Apparatus

The Ammis ImageStream X Mk II imaging cytometer (Luminex, Austin, TX, USA) was employed to characterize cultured cells and functionalized MBs. The LICOR Oddyssey^{TM} Scanner was employed to visualized WB bands by infrared labelling. A NanoSight NS300 nanoparticle analyzer (Malvern Instruments, UK) was employed to

characterize EVs size and EVs concentration. Zeiss GEMINI high-resolution Scanning Electron Microscope (SEM) was employed to characterize the functionalized MBs. Chromatogram of the EVs isolation was performed by A260/A280 with NanoDrop™ 2000c (Thermo Fisher Scientific, Inc.,Wilmington, DE, USA). Colorimetric detection was realized using NanoQuant infinite M200 Pro (TECAN, Switzerland). Sensit Smart Potentiostat (Palm Sens, Netherlands) was used for amperometric detection.

2.3. Preparation of the anti-EpCAM functionalized MBs

A 3 µL-aliquot of the homogenized HOOC-MBs (Dynabeads^{TM}) suspension was washed twice with MES buffer for 10 min (25 °C, 950 rpm). Thereafter, the activation of the MBs surface carboxylic groups was carried out by using 25 µL of a freshly prepared EDC/sulfo-NHS solution for 35 min (25 °C, 950 rpm). After washing, the activated MBs were incubated for 30 min (25 °C, 950 rpm) with 25 µL of a 10 µg mL^{-1} of anti-EpCAM (ab223582 Abcam, UK) solution prepared in the MES buffer. This capture antibody is suitable for flow cytometry and recognizes the extracellular fraction of the protein. Subsequently, the residual activated groups were blocked by incubating in a 1.0 M ethanolamine solution for 1 h (25 °C, 950 rpm). Finally, the anti-EpCAM - MBs were washed once with 0.1 M Tris-HCl buffer (pH 7.2), twice with PBS, and stored at 4 °C in sterilized PBS solution until their use.

2.4. Cell culture

All cultured cell lines were obtained from the ATCC trough the University of Granada Cell Line Bank. The LNCAP and PC-3 from prostate adenocarcinoma adherent cells were cultured in RPMI medium, supplemented with 10 % of Fetal Bovine Serum (FBS) and 1 % of penicillin/streptomycin solution (P/S) in incubators at 37 ºC and 5% of CO_2. Jurkat cell line from acute leukaemia was cultured in suspension in RPMI medium supplemented with 10% of FBS and 1 % of P/S in incubators at 37 ºC and 5% of CO_2. Cell were growth

until confluence in T-175 flasks and later, incubated for 48 hr in Media Without FBS before starvation of EVs.

2.5. EVs isolation

EVs isolation was performed form 2 mL of plasma of 2 mL of 100 KD Tangential Flow Filtration concentrated media. Sample was centrifuged at 300 g during 5 min, supernatant was recovered and subsequently centrifuged at 2000 g during 15 min. Then, the obtained supernatant was fractioned by size exclusion chromatography (SEC) columns with 35 nm pore size (qEV2 Columnns, Izon Size, France). Fractions were collected in 2 mL tubes and fractions 8, 9 and 10 were pooled and employed for subsequent analysis.

2.6. WBs analysis

Total protein was extracted from cells or EVs using a lysis buffer containing 0.2 % Triton X-100, 50 mM Hepes (pH 7.5), 100 mM NaCl, 1 mM $MgCl_2$, 50 mM NaF, 0.5 mM Na_3VO_4, 20 mM β-glycerophosphate, 1 mM phenylmethylsulfonyl fluoride, and protease inhibitors (Roche, Germany) [24]. The lysates were centrifuged at 15,000 × g for 15 min at 4 °C to remove insoluble material. Protein concentrations were then determined using a BCA Protein Assay Kit (Thermo Fisher, Waltham, MA, USA). The lysates were mixed with a sample buffer containing β-mercaptoethanol, heated to 95 °C, and subjected to electrophoresis on 4–12 % Bis-Tris polyacrylamide gels (Bio-Rad, UK). Proteins were transferred to nitrocellulose membranes (Bio-Rad, UK). The membranes were blocked with non-fat milk and then incubated overnight at 4 °C with the following primary antibodies: mouse anti-CD81 (1:1000, clone 1A12, Santa Cruz, USA), mouse anti-HSC70 (1:1000, clone B-6, Santa Cruz, USA) and anti-EpCAM (1:1000, EPR20532, abcam biotech, UK) as described in a previous work [25]. Following primary antibody incubation, membranes were incubated for 1 hour with secondary antibodies: IRDye 800

donkey anti-mouse (1:10.000, LI-COR Biosciences, UK). Finally, membrane was washed and scanned employing Odyssey Scanner (LICOR Biosciences, UK).

2.7. Nanoparticle tracking analysis

The size distribution and concentration of EVs were determined using a NanoSight NS300 nanoparticle analyzer (Malvern Instruments, UK) equipped with a 405 nm laser. The camera level was set to 15–16, and all post-acquisition settings were set to automatic, except for the detection threshold, which was fixed at 6. Using the script control function, three 30-second videos were recorded for each sample. The data was analyzed with NTA 3.1 as previously described [25].

2.8.Transmission electronic microscopy

EVs were adsorbed onto active carbon-coated grids for 10 min, then washed and fixed for 15 min in a solution containing 2 % paraformaldehyde and 0.2 % glutaraldehyde. The grids were briefly rinsed and immediately transferred to drops of uranyl methyl cellulose (pH 4.0) on a cooled metal plate for 5 min. They were then picked up and allowed to dry at room temperature. Finally, the grids were examined using a FEI Tecnai™ F20 transmission electron microscope (TEM).

2.9. Blood sample collection

The study received approval from the Ethical Committee of Virgen de las Nieves University Hospital and adhered to the principles outlined in the Declaration of Helsinki. Written informed consent was obtained from all participants for the use of their samples. Patients and non cancer controls were recruited and monitored in the hospital's Urology and Oncology Departments. All they are patients of the urology department and were recruited according to the inclusion criteria described at the supplementary materials. The clinical data of the study participants are provided in Table S1 and S2.

2.10. MBs-EpEVs-HRP complexes preparation

Isolated EVs were blocked with 5% BSA and 1% FcR (Fc receptor) blocking reagent for 5 min and then incubated with Anti-EpCAM functionalized MBs and Anti-CD81 biotinylated antibody (ab239238, Clone [M38], Abcam, UK) for 15 min at room temperature in a 1,5 mL tube. Similarly to the capture antibody, this detection antibody is recommended for flow cytometry and was produced using a cell preparation containing the CD81 protein. Then, the complex was washed twice with PBS placing it in a magnetic field. Then, complexes are resuspended with 100 µl of PBS and incubated during 5 min. with HRP streptavidin as indicated. Finally, complexes were washed twice and employed for either colorimetric or amperometric measurements.

2.11. Colorimetric analysis by Immune magnet ELISA

The MB-EpEVs-HRP complexes were resuspended in 100 µl of 3,3,5,5 Tetramethylbenzidine (TMB) solution during indicated times. Then, complexes were read at NanoQuant infinite M200 Pro with an absorbance of 650 nm without stop solution and at 450 nm when stop solution was added.

2.12. Amperometric measurements

The MBs-EpEVs-HRP complexes were droplet on WE surface of a SPCE (Palm Sens) previously attached in the back to a magnet, the SPCE was connected to the potentiostat (Palm Sens) and placed into an electrochemical cell that contained 10 mL of 0.05 M PBS (pH 6.0) and 1.0 mM of HQ. A detection potential value of - 0.2 V related to the Ag electrode was selected for the measurements when 50 µL of a 0.1 M H_2O_2 solution is added. Signal was calculated as the difference between the steady state and the background current, being the value the mean of three measurements. Scheme 1 illustrates the detection principle of the developed method.

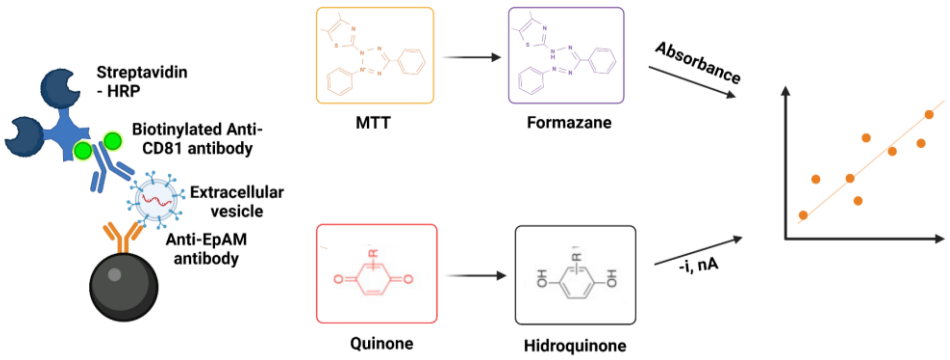

Scheme 1. *Representation of detection principle of the developed method.*

3. Results and Discussion

3.1. Characterization of the EVs isolation methodology

After isolating the EVs fractions, the purity of the EVs was analyzed in NanoDrop™ 2000c, by A260/A280. These parameters were used to construct the chromatogram (Fig. 1A). The result was 4 protein peaks, where peaks 1 and 2 were enriched in EVs (Fig. 1B), and to a lesser extent peaks 3 and 4.

The peaks enriched in EVs were characterized by NTA and TEM, where the mean particle size was 113.9 nm and a mode of 77.7 nm (Fig. 1C), typical size of exosomes. Fig. 1D shows the EVs structure, with presence of a double membrane and an electrodense content.

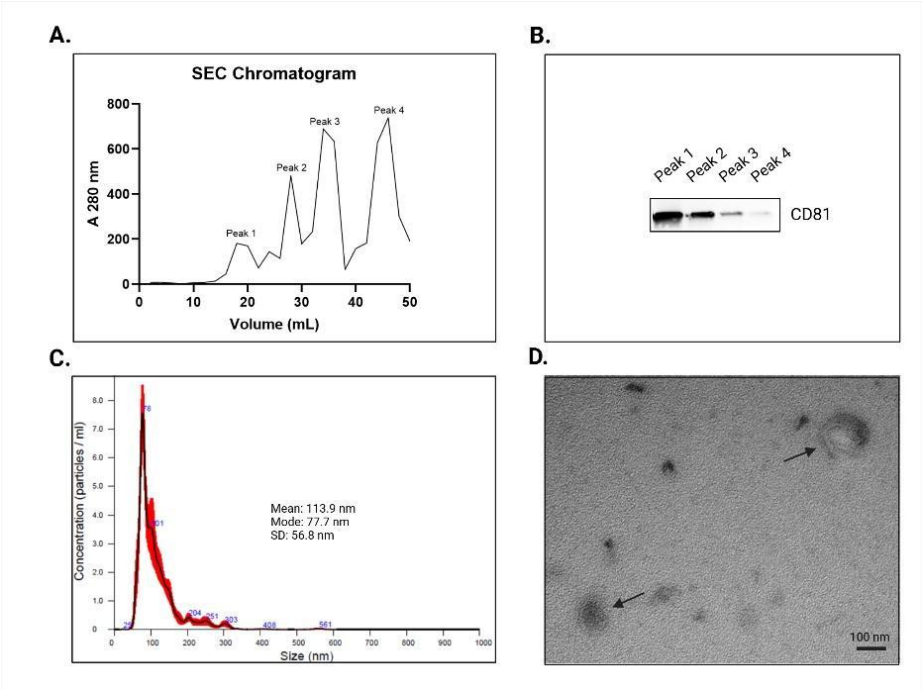

Figure 1. *A) Chromatogram of the protein profiles obtained by SEC. B) Presence of CD81 in each of the 4 peaks, quantified by western blot. C) Analysis of the distribution and size of particles present in the sample by NTA. D) Extracellular vesicles observed by TEM.*

3.2. MBs characterization and functionalization

The MBs were functionalized with monoclonal antibodies against human EpCAM. The functionalized MBs were characterized using scanning electron microscopy (SEM), showing a uniform coating and consistent bead morphology (Fig. 2A) Additionally, the correct binding of EpCAM-positive EVs to the functionalized MBs was validated by a kinetic colorimetric assay, with CD81 beads as a positive control (Fig. 2B). EpCAM-functionalized MBs recovered more EVs from the PC-3 cell line, whose membranes and EVs are enriched in EpCAM (Supplementary information, Fig. S1), followed by LNCaP. No EVs were captured from the Jurkat line, where EpCAM expression is almost nil (Fig. 2C). These results confirm that the functionalized MBs effectively captured EpCAM-positive EVs, ensuring specificity and reliability in the subsequent electrochemical detection assays.

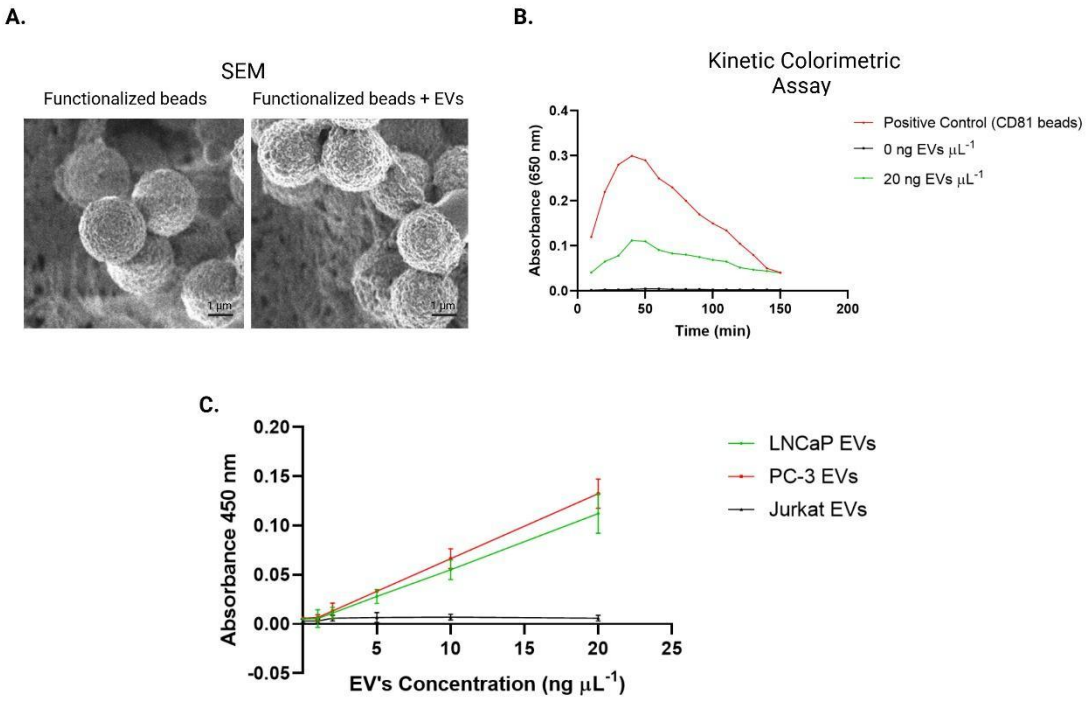

Figure 2. *A) Representative SEM micrographs of the DynabeadsTM functionalized, without and with EVs. B) Kinetic Colorimetric Assay of different EVs concentrations. C) Linear representation of the absorbance of different EVs concentrations from three cell lines.*

3.3. Optimization of experimental variables

A control dilution of 5 ng mL^{-1} EpEVs from the PC-3 cell line was used for the optimization of experimental variables. The variables optimized were concentrations and incubation times of EpCAM and biotinylated CD81 antibodies (Ab), and streptavidin-HRP. The signal measure was electrochemical.

The concentration of EpCAM Ab was varied from 0 to 40 µg mL^{-1}. The highest response was observed at 10 µg mL^{-1}, indicating that this concentration provided optimal antibody coverage without saturation effects (Fig. 3A). The best incubation time of EpCAM Ab was 30 min. (Fig. 3B). For biotinylated CD81 Ab concentration, the signal increased significantly at 0.25 µg mL^{-1} (Fig. 3C), and with an optimal incubation time of 45 min (Fig. 3D). The dilution of strep-HRP testing shown a peak response at 50 ng mL^{-1} (Fig. 3E). The fittest incubation time was 15 min (Fig. 3F). Based on this result the

optimal time for the immune complex formation was 1 hour. For subsequent experiments, we determined the optimal time point for signal measurement and found that the greatest differences between the curves occurred after 1 minute (Fig. 3G).

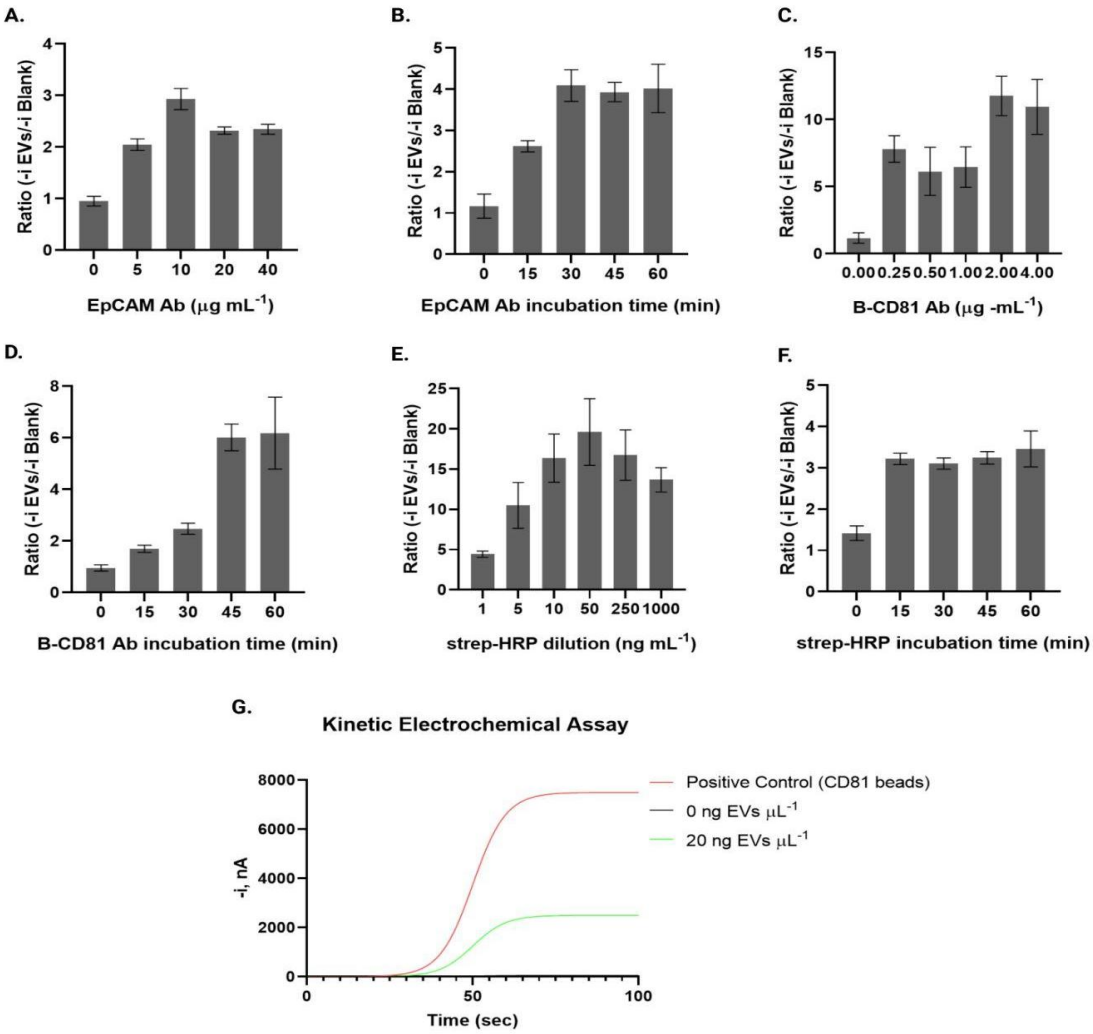

Figure 3. *Bar graphics representing the mean values of three technical replicates. Errors bars represent the standard deviation. Here, we identified (A) the optimal concentration of capture antibody anti-EpCAM, (B) the optimal incubation time of anti-EpCAM Ab, (C) the best concentration of anti-CD81 biotinylated antibody, (D) the optimal incubation time of anti-CD81 (E) the fittest concentration of strep-HRP and (F) the best incubation time of strep-HRP. (0 indicates no antibody added or no incubation). G) Kinetic Electrochemical Assay of different EVs concentrations.*

3.4. Quantitative determination of EpEVs by the electrochemical method

Next, our optimized Immune-Magnet ELISA was used to compare the performance of our electrochemical chip. This Assay shows absorbance changes against the

corresponding EpEVs concentration of serially diluted samples. The linear regression equation was $A = 0.003 + 0.006 \times C_{EpEVs}$, with linear regression coefficient r = 0.947 and CV of 6.54% for the determination of 10 ng μL^{-1} EpEVs (five replicates), a lower precision than obtained with the proposed immunoplatform.

The electrochemical method was used to determine the current of serial EpEVs dilutions under the optimized conditions. The linear regression equation was $i\ (nA) = 8.18 + 119.80 \times C_{EpEVs}$, with linear regression coefficient r = 0.998. A linear relation was observed between the concentration range 0–20 ng μL^{-1}. The coefficient of variation (CV) for the determination of 10 ng μL^{-1} EpEVs biomarker was 3.81% (five replicates). The amperometric response increased proportionally with the concentration of the EpEVs biomarker, indicating a direct linear relationship between the concentration of EpCAM-positive EVs and the intensity of the measured current (Fig. 4A).

The limit of detection (LOD) was defined as the lowest concentration yielding a signal three times the standard deviation of the blank. The LOD was 5 ng μL^{-1} for the ELISA test, and the LOD of 0.4 ng μL^{-1} for the present analytical method.

The proposed dual signal electrochemical method was compared with a commercial ELISA, using both to analyse biological samples with different EpEVs levels. The slopes obtained were close to 1, indicating a good correlation of the two methods (Fig. 4B). Moreover, when we employed EVs spiked healthy donor`s plasma, perfect correlation was observed between electric signal and concentration of spiked EVs from both, LNCaP and PC3 cells. Interestingly, EVs from cells who showed higher level of EpCAM has an increased slope (Fig. 4C). As it is a method of capture by EpCAM and quantification by CD81, EVs from cells with higher expression of epCAM will have a higher signal at the same vesicle concentration.

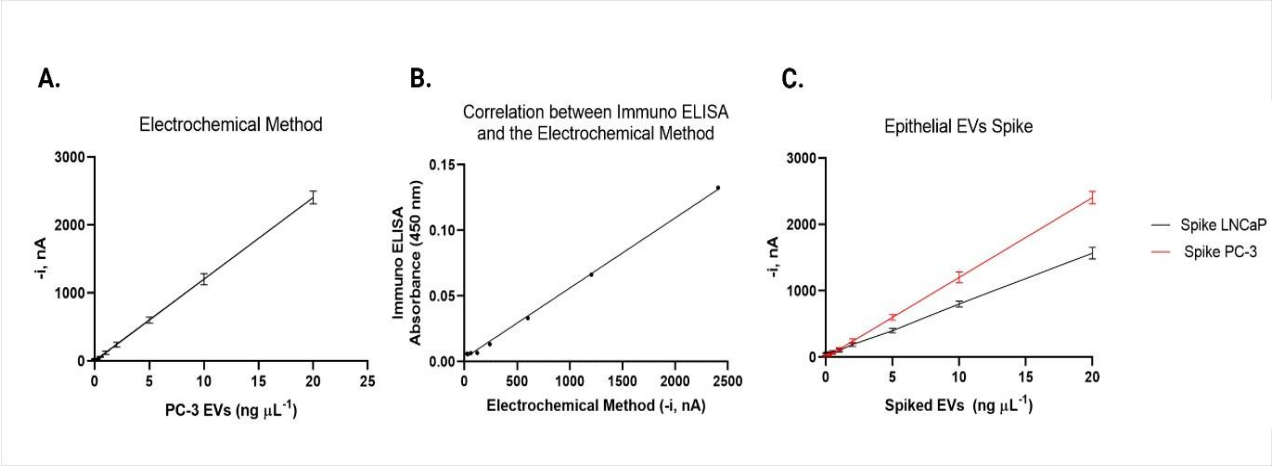

Figure 4. *A) Calibration curve of proposed analytical method. B) Correlation between electrochemical method and commercial ELISA. C) Correlation between spiked EVs from LNCaP and PC-3 cells and current intensity.*

3.5. Clinical performance of the electrochemical quantification of EpCAM + EpEVs

Current values associated with EpEVs are observed to be significantly higher in patients with PCa compared to healthy donors (Fig. 5A), differences between pooled samples from controls and patients are also evident (Fig. 5B). The ROC curve shows a high sensitivity and specificity for EpEVs as a biomarker, with an area under the curve (AUC) of 0.9210, and a standard error of 0.03304 (Fig. 5C).

However, by combining EpEVs with PSA values, an improvement in sensitivity and specificity is achieved. The AUC increases to 0.9700, with a standard error of 0.01696, indicating that the combination of both biomarkers provides a more robust diagnostic method (Fig. 5D).

In addition, a positive linear correlation was observed between PSA values and EpEVs current signal (Fig. 5E). Likewise, a significant decrease in EpEVs values was observed after 6 weeks, possibly due to treatment or intervention in prostate cancer patients (Fig 5F). This suggests that EpEVs could be used not only as a diagnostic biomarker, but also as an indicator of therapeutic response, an essential factor in the

follow-up of therapeutic outcomes and a highly relevant tool for the longitudinal monitoring of patients with recurrence risk.

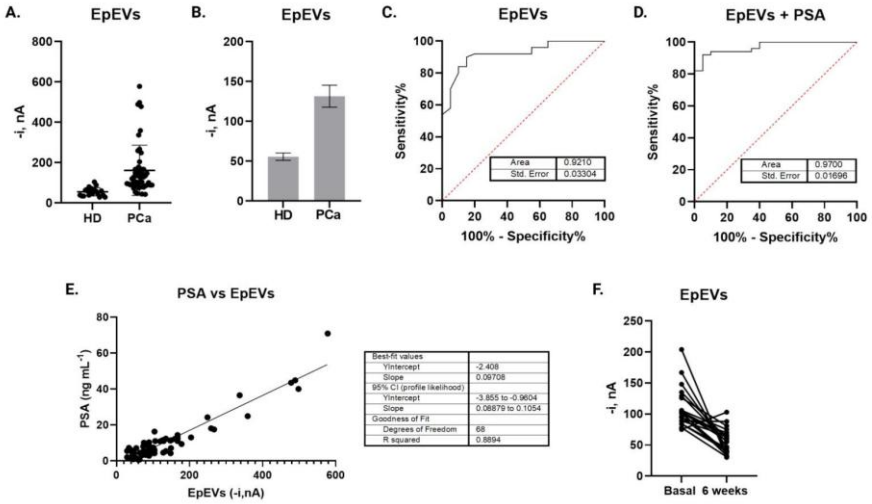

Figure 5. *A) EVs current intensity in healthy donors and prostate cancer patients. B) EVs current intensity of a pool of samples from Healthy Donors (HD) and Prostate Cancer (PCa) patients, 10 samples per each pool. C) ROC curve and AUC for EpEVs. D) ROC curve and AUC for EpEVs + PSA. E) Linear correlation between PSA concentration levels and EpEVs current intensity. F) Current intensity of EpEVs for PCa patients at basal time and at 6 weeks of the disease.*

This study demonstrates the potential of a dual-mode immunosensor for the detection of epithelial-derived extracellular vesicles (EpEVs) as a novel biomarker for prostate cancer (PCa) diagnosis. The use of EpCAM as a capture marker and CD81 as a detection marker effectively distinguishes EpCAM-positive EVs, which are enriched in PCa cell lines. These findings suggest a significant step forward in the early diagnosis of PCa, offering improvements over conventional methods[26].

Early diagnosis is critical in prostate cancer management, as it enables timely intervention, potentially improving patient outcomes and survival rates[3], [27]. Current clinical practices rely heavily on prostate-specific antigen (PSA) testing, which, while valuable, is limited by false positives and lack of specificity[6]. Many conditions, including benign prostatic hyperplasia and prostatitis, can lead to elevated PSA levels,

complicating the differentiation of malignant and non-malignant cases[4]. The inclusion of EpEVs as an additional biomarker significantly enhances diagnostic precision[28]–[30], as evidenced by the improved area under the curve (AUC) when combining EpEVs with PSA measurements.

This dual-biomarker approach not only enhances early detection but also could reduce the unnecessary biopsies or overtreatment, benefiting patients and reducing healthcare burdens[31], [32]. The electrochemical platform described in this work offers several advantages over the traditional ELISA approach. With a lower limit of detection (LOD) and better precision, the electrochemical assay demonstrates enhanced sensitivity to EpEVs, even at low concentrations. The strong correlation between the two methods further validates the electrochemical approach, emphasizing its reliability and robustness.

Additionally, the assay's linear response to EpCAM-positive EVs concentrations under optimized conditions provides a quantifiable and reproducible measurement. This property is crucial for clinical applications, particularly for monitoring disease progression or response to therapy, as shown in the significant decrease in EpEVs observed in treated PCa patients.

4. Conclusions

The immuno-electrochemical detection of EpCAM-positive EVs offers a promising advancement in prostate cancer diagnostics. By combining EpEV detection with PSA measurements, this study demonstrates improved sensitivity and specificity for early diagnosis. Furthermore, the platform's ability to monitor therapeutic responses positions EpEVs as a versatile biomarker for both diagnostics and prognostics. These findings underscore the importance of integrating innovative EV-based methods into routine clinical workflows, paving the way for more precise and personalized PCa management.

Declaration of competing interests

The authors declare that they have no known competing financial interests or personal relationships that could have appeared to influence the work reported in this paper.

Credit authorship contribution statement

Emiliano Felici and Coral González-Martínez: Investigation, Methodology, Writing - original draft. **Emiliano Felici and Sheila Gato Zambrano:** Investigation, Data curation, Validation, Writing - original draft. **Teresa Valero Griñán, Sirley V. Pereira, Francisco Gabriel Ortega and Martín A. Fernández-Baldo:** Resource, Visualization, Supervision, Funding acquisition. **Teresa Valero Griñán, Sirley V. Pereira, Francisco Gabriel Ortega and Martín A. Fernández-Baldo:** Conceptualization, Supervision, Funding acquisition, Writing - review & editing, Project administration.

Acknowledgments

Universidad Nacional de San Luis (PROICO 02-2220), Agencia Nacional de Promoción Científica y Tecnológica (PICT-2021-GRF-TI-00136). Consejo Nacional de Investigaciones Científicas y Técnicas (CONICET) (PIP-11220200100033CO). Instituto de Salud Carlos III (ISCIII) (PI22_01275, CP23/00134, DTS23_00030). Universidad de Granada (P32/22/02).

References

[1] H. Sung *et al.*, "Global Cancer Statistics 2020: GLOBOCAN Estimates of Incidence and Mortality Worldwide for 36 Cancers in 185 Countries," *CA. Cancer J. Clin.*, vol. 71, no. 3, pp. 209–249, 2021, doi: 10.3322/caac.21660.

[2] K. J. L. Bell, C. Del Mar, G. Wright, J. Dickinson, and P. Glasziou, "Prevalence of incidental prostate cancer: A systematic review of autopsy studies," *Int. J. cancer*, vol. 137, no. 7, pp. 1749–1757, Oct. 2015, doi: 10.1002/IJC.29538.

[3] R. C. N. van den Bergh, S. Loeb, and M. J. Roobol, "Impact of Early Diagnosis of Prostate Cancer on Survival Outcomes," *Eur. Urol. Focus*, vol. 1, no. 2, pp. 137–146, Sep. 2015, doi: 10.1016/J.EUF.2015.01.002.

[4] S. P. Balk, Y. J. Ko, and G. J. Bubley, "Biology of prostate-specific antigen," *J. Clin. Oncol.*, vol. 21, no. 2, pp. 383–391, Jan. 2003, doi: 10.1200/JCO.2003.02.083.

[5] A. Madej, J. Wilkosz, W. Rózański, and M. Lipiński, "Complication rates after prostate biopsy according to the number of sampled cores," *Cent. Eur. J. Urol.*, vol. 65, no. 3, p. 116, 2012, doi: 10.5173/CEJU.2012.03.ART3.

[6] S. Saini, “PSA and beyond: alternative prostate cancer biomarkers,” *Cell. Oncol.*, vol. 39, no. 2, pp. 97–106, Apr. 2016, doi: 10.1007/S13402-016-0268-6/METRICS.

[7] G. Raposo and W. Stoorvogel, “Extracellular vesicles: exosomes, microvesicles, and friends.,” *J. Cell Biol.*, vol. 200, no. 4, pp. 373–83, Feb. 2013, doi: 10.1083/jcb.201211138.

[8] R. Xu, A. Rai, M. Chen, W. Suwakulsiri, D. W. Greening, and R. J. Simpson, “Extracellular vesicles in cancer — implications for future improvements in cancer care,” *Nat. Rev. Clin. Oncol.*, vol. 15, no. 10, pp. 617–638, Oct. 2018, doi: 10.1038/s41571-018-0036-9.

[9] Y. Vinik *et al.*, “Proteomic analysis of circulating extracellular vesicles identifies potential markers of breast cancer progression, recurrence, and response,” *Sci. Adv.*, vol. 6, no. 40, pp. 1–12, 2020, doi: 10.1126/sciadv.aba5714.

[10] D. D. Taylor, W. Zacharias, and C. Gercel-Taylor, “Exosome isolation for proteomic analyses and RNA profiling.,” *Methods Mol. Biol.*, vol. 728, pp. 235–46, Jan. 2011, doi: 10.1007/978-1-61779-068-3_15.

[11] N. Sahraei, M. Mazloum-Ardakani, A. Khoshroo, F. Hoseynidokht, J. Mohiti, and A. Moradi, “Electrochemical system designed on a paper platform as a label-free immunosensor for cancer derived exosomes based on a mesoporous carbon foam- ternary nanocomposite,” *J. Electroanal. Chem.*, vol. 920, no. June, 2022, doi: 10.1016/j.jelechem.2022.116590.

[12] S. Cinti *et al.*, “Paper-based electrochemical device for early detection of integrin αvβ6 expressing tumors,” *Commun. Chem.*, vol. 7, no. 1, pp. 1–9, 2024, doi: 10.1038/s42004-024-01144-z.

[13] D. G. Mathew, P. Beekman, S. G. Lemay, H. Zuilhof, S. Le Gac, and W. G. Van Der Wiel, “Electrochemical Detection of Tumor-Derived Extracellular Vesicles on Nanointerdigitated Electrodes,” *Nano Lett.*, vol. 20, no. 2, pp. 820–828, 2020, doi: 10.1021/acs.nanolett.9b02741.

[14] J. V. Jokerst *et al.*, “A magnetic bead-based sensor for the quantification of multiple prostate cancer biomarkers,” *PLoS One*, vol. 10, no. 9, pp. 1–15, 2015, doi: 10.1371/journal.pone.0139484.

[15] Y. Zhou *et al.*, “Tumor biomarkers for diagnosis, prognosis and targeted therapy,” *Signal Transduct. Target. Ther. 2024 91*, vol. 9, no. 1, pp. 1–86, May 2024, doi: 10.1038/s41392-024-01823-2.

[16] W. Li *et al.*, “Noninvasive Diagnosis and Molecular Phenotyping of Breast Cancer through Microbead-Assisted Flow Cytometry Detection of Tumor-Derived Extracellular Vesicles,” *Small Methods*, vol. 2, no. 11, Nov. 2018, doi: 10.1002/SMTD.201800122.

[17] X. Shi, X. Zhao, J. Xue, and E. Jia, “Extracellular vesicle biomarkers in circulation for colorectal cancer detection: a systematic review and meta-analysis,” *BMC Cancer*, vol. 24, no. 1, Dec. 2024, doi: 10.1186/S12885-024-12312-8.

[18] S. Xiao *et al.*, “Accurate and Convenient Lung Cancer Diagnosis through Detection of Extracellular Vesicle Membrane Proteins via Förster Resonance

Energy Transfer," *Nano Lett.*, vol. 23, no. 17, pp. 8115–8125, Sep. 2023, doi: 10.1021/ACS.NANOLETT.3C02193/ASSET/IMAGES/LARGE/NL3C02193_0005.JPEG.

[19] D. R. Shaffer *et al.*, "Circulating tumor cell analysis in patients with progressive castration-resistant prostate cancer.," *Clin. Cancer Res.*, vol. 13, no. 7, pp. 2023–9, Apr. 2007, doi: 10.1158/1078-0432.CCR-06-2701.

[20] F. S. Felix and L. Angnes, "Electrochemical immunosensors - A powerful tool for analytical applications," *Biosens. Bioelectron.*, vol. 102, pp. 470–478, Apr. 2018, doi: 10.1016/J.BIOS.2017.11.029.

[21] F. G. Ortega-Sanchez *et al.*, "Microfluidic systems in extracellular vesicles single analysis. A systematic review," *TrAC - Trends Anal. Chem.*, vol. 159, 2023, doi: 10.1016/j.trac.2023.116920.

[22] M. Pastucha, Z. Farka, K. Lacina, Z. Mikušová, and P. Skládal, "Magnetic nanoparticles for smart electrochemical immunoassays: a review on recent developments," *Mikrochim. Acta*, vol. 186, no. 5, May 2019, doi: 10.1007/S00604-019-3410-0.

[23] F. G. Ortega *et al.*, "Microfluidic amperometric immunosensor based on porous nanomaterial towards claudin7 determination for colorectal cancer diagnosis," *Talanta*, vol. 251, no. May 2022, 2023, doi: 10.1016/j.talanta.2022.123766.

[24] B. T. Hennessy *et al.*, "A Technical Assessment of the Utility of Reverse Phase Protein Arrays for the Study of the Functional Proteome in Non-microdissected Human Breast Cancers.," *Clin. Proteomics*, vol. 6, no. 4, pp. 129–51, Dec. 2010, doi: 10.1007/s12014-010-9055-y.

[25] F. G. Ortega *et al.*, "Interfering with endolysosomal trafficking enhances release of bioactive exosomes," *Nanomedicine Nanotechnology, Biol. Med.*, vol. 20, 2019, doi: 10.1016/j.nano.2019.102014.

[26] S. Khaksari, K. Abnous, F. Hadizadeh, M. Ramezani, S. M. Taghdisi, and S. A. Mousavi Shaegh, "Signal amplification strategies in biosensing of extracellular vesicles (EVs)," *Talanta*, vol. 256, no. December 2022, p. 124244, 2023, doi: 10.1016/j.talanta.2022.124244.

[27] E. Dezhakam *et al.*, "Electrochemical biosensors in exosome analysis; a short journey to the present and future trends in early-stage evaluation of cancers," *Biosens. Bioelectron.*, vol. 222, no. December 2022, p. 114980, 2023, doi: 10.1016/j.bios.2022.114980.

[28] J. Tan, Y. Wen, and M. Li, "Emerging biosensing platforms for quantitative detection of exosomes as diagnostic biomarkers," *Coord. Chem. Rev.*, vol. 446, p. 214111, 2021, doi: 10.1016/j.ccr.2021.214111.

[29] Y. Teng, W. Li, and S. Gunasekaran, "Biosensors based on single or multiple biomarkers for diagnosis of prostate cancer," *Biosens. Bioelectron. X*, vol. 15, no. September, p. 100418, 2023, doi: 10.1016/j.biosx.2023.100418.

[30] H. Xie *et al.*, "Extracellular vesicles based electrochemical biosensors for detection of cancer cells: A review," *Chinese Chem. Lett.*, vol. 31, no. 7, pp. 1737–1745, 2020, doi: 10.1016/j.cclet.2020.02.049.

[31] E. Felici *et al.*, "Microfluidic Platform Integrated with Carbon Nanofibers-Decorated Gold Nanoporous Sensing Device for Serum PSA Quantification," *Biosensors*, vol. 13, no. 3, 2023, doi: 10.3390/bios13030390.

[32] W. Feng, P. Xu, M. Wang, G. Wang, G. Li, and A. Jing, "Electrochemical Micro-Immunosensor of Cubic AuPt Dendritic Nanocrystals/Ti3C2-MXenes for Exosomes Detection," *Micromachines*, vol. 14, no. 1, 2023, doi: 10.3390/mi14010138.

Supplementary Information:

Electrochemical immunoplatform for the quantification of epithelial extracellular vesicles applied to prostate cancer diagnosis

Emiliano Felici[† 1], Coral González-Martínez[† 2, 3, 4], Teresa Valero Griñán [2, 4, 5,*], Sheila Gato-Zambrano [6], Sirley V. Pereira [1], Martín A. Fernández-Baldo [1,*], Francisco G. Ortega-Sanchez [2,3,4]

[1] *Universidad Nacional de San Luis, Facultad de Química, Bioquímica y Farmacia, Instituto de Química de San Luis, INQUISAL (UNSL - CONICET), Av. Ejército de los Andes 950, San Luis D5700BWS, Argentina.*

[2] *GENYO, Centre for Genomics and Oncological Research, Pfizer/University of Granada/Andalusian Regional Government, PTS Granada, Avenida de la Ilustración 114, Granada 18016, Spain.*

[3] *Laboratory of Genetic Identification, Legal Medicine and Toxicology Department, Faculty of Medicine, University of Granada, Avenida de la Investigación 11, Granada 18071, Spain.*

[4] *Instituto de Investigación Biosanitaria ibs.GRANADA, Avda. de Madrid, 15, Granada 18012, Spain.*

[5] *Department of Medicinal and Organic Chemistry, School of Pharmacy, University of Granada, Campus Cartuja s/n, 18071 Granada, Spain.*

[6] *Seliver Group, Institute of Biomedicine of Seville/ /Hospital, Universitario Virgen del Rocío/CSIC/Universidad de Sevilla, Sevilla, Spain.*

[†] Equal Contribution.

Authors to whom correspondence should be addressed: (e-mail) mbaldo@unsl.edu.ar or tvalero@go.ugr.es

Supplementary Material 1

1.1 Recruited cohorts. Inclusion Criteria

Control Cohort (Non-Cancer Urology Patients):

Male individuals aged 45–75 years who were evaluated at the urology department for benign urological conditions, such as benign prostatic hyperplasia (BPH), urinary tract infections, kidney stones, or prostatitis. All participants in this group had no current or previous diagnosis of cancer of any type and no family history of prostate cancer. Patients with abnormal PSA levels or suspicious findings on digital rectal examination (DRE) were excluded unless cancer had been definitively ruled out via negative biopsy.

Prostate Cancer Cohort (Localized, Pre-Surgery):

Male patients aged 55–77 years with a histologically confirmed diagnosis of localized prostate cancer (clinical stage T2–T3) scheduled for radical prostatectomy. All individuals had not yet received any treatment (e.g., surgery, radiotherapy, or hormone therapy) at the time of sample collection. Clinical data including PSA levels, Gleason score, prostate volume, DRE findings, and biopsy results were recorded prior to surgery.

Table S1. Patient characteristics:

Age, years. Media (range)	66,36 (46-77)
Nudes invasion	24 (52,2 %)
Seminal Invasion	10 (20%)
Gleason	
≤ 6	8 (162%)
7	27 (54%)
≥ 8	15 (30%)
Pathological Stages	
pT2	25 (54%)
pT3	23 (46%)

Table S2. Controls characteristics

Age, years. Media (range)	57 (45-70)
Urological Disorder	
Benign prostatic hypertrophy	7 (35%)
Routine screening	5 (25%)
Hematuria	3 (15%)
Erectile dysfunction	1 (5%)
Urinary tract infection	2 (10%)
Kidney stones	2 (10%)

Supplementary Figure 1.

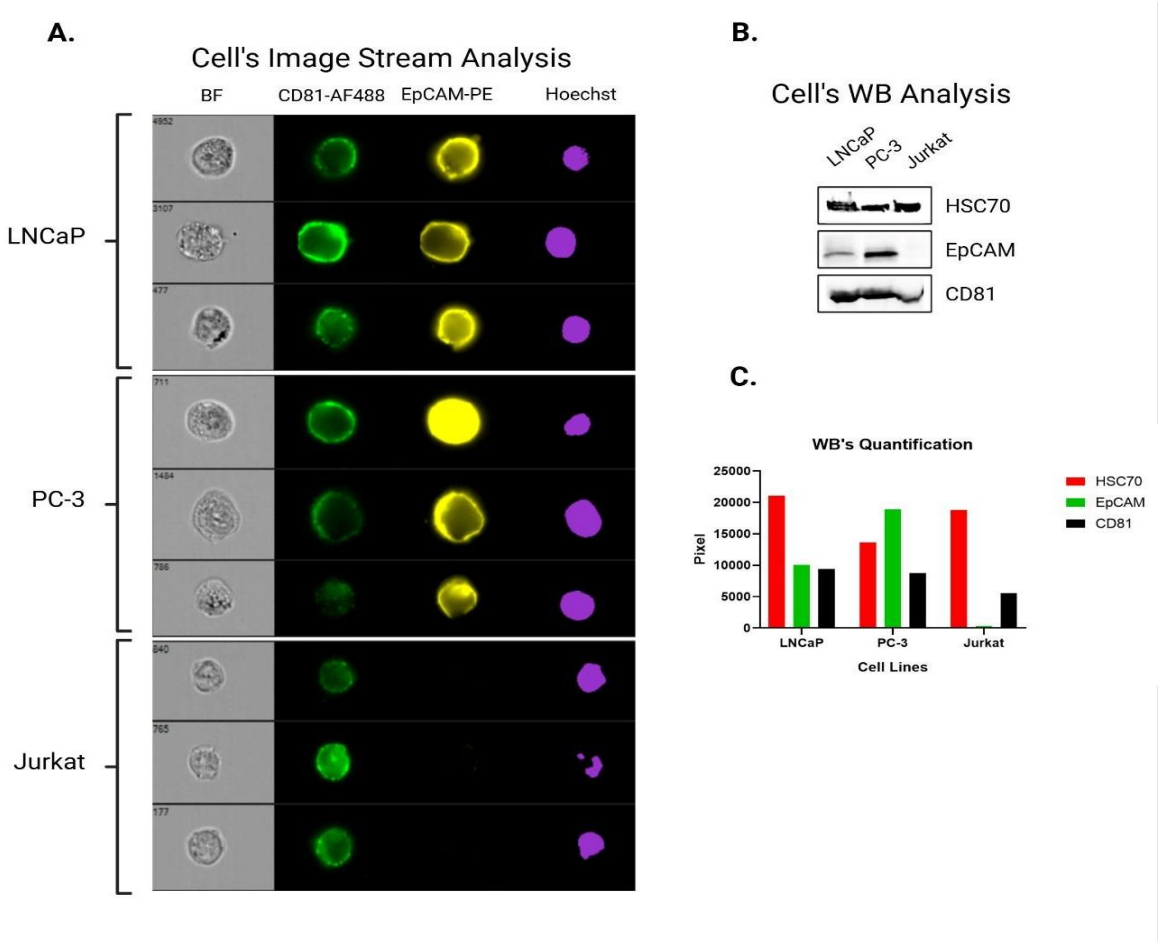

Supplementary Figure 1: *A) Image stream analysis of prostate cancer (LNCap and PC-3) and leukaemia (Jurkat) cells lines where CD81(green), EpCAM (Yellow), and Nucleus (purple) were visualized (BF: Bright Field). B) Western Blot Analysis of the three cell lines for the HSC70, EPCAM and CD81 levels. C) Image J quantification of the WB analysis.*

Graphical Abstract